



Research on deformation prediction and error compensation in precision turning of micro-shafts

Chenxu Li¹ · Xibin Wang² · Pei Yan² · Zhongke Niu³ · Shiqi Chen¹ · Li Jiao²

Received: 15 December 2019 / Accepted: 9 August 2020 / Published online: 25 August 2020
© Springer-Verlag London Ltd., part of Springer Nature 2020

Abstract

The precision turning process has attracted enormous interest in the standardized and mass production of micro-shafts because it produces more efficiency and lower cost compared with the electrical-discharge machining method and micro-machining method. However, there are many critical factors that influence the dimensional accuracy of micro-shafts, such as the error of workpiece deformation, cutting force, and tool setting error. In this paper, a novel error compensation method was proposed to improve the dimensional accuracy of micro-shafts manufactured with the conventional precision machine tool, based on the constant force cutting method and tool path planning. Firstly, a cutting force model was established considering the effect of the tool nose radius, and the finite element method was used to simulate the turning process and predict the workpiece deformation. Secondly, an error analysis model was created by taking tool setting error, workpiece deformation error, and multi-process cumulative error into account, and the optimized tool path and cutting parameters were obtained. Finally, a series of turning experiments were carried out to verify the error compensation strategy and the cutting force model. The results show that the dimensional error of the micro-shafts with a large length-diameter ratio ($l = 5$ mm, $d = 0.4$ mm) can be reduced by 90% by means of the proposed error compensation strategy. In addition, the maximum prediction error of cutting forces is less than 8.6%, and the effect of cutting parameters on cutting forces can be concluded as “feed rate > depth of cut > spindle speed.”

Keywords Micro-shafts · Precision turning · Error compensation · Constant force cutting · Tool path planning · FEA method

1 Introduction

Recently, the requirement for micro-scale components and products is increasing rapidly, particularly in the fields of electronics, communications, optics, avionics, medicine, automobiles, and so on [1–3]. Typical applications of such miniaturized products include micro-engines, micro-reactors, micro-heat exchangers, medical implants, drug delivery devices, and diagnostic devices [4, 5]. Various manufacturing techniques such as electrodischarge machining, ion beam machining, laser beam

machining, and photolithography have been proposed. However, the abovementioned micro-machining methods are limited to planar geometries and have poor productivity and relatively high cost [6]. Mechanical micro-machining has significant advantages in comparison with other machining techniques in terms of workpiece complexity, material diversity, energy consumption, and cost [7]. The family of aluminum alloys are always used for micro-parts manufacturing because of their superior characteristics such as recyclability, conductivity, processability, non-magnetization, low density, and corrosion resistance [8, 9]. Micro-shaft (0.1–1 mm) is one of the important micro-parts which have high machining accuracy requirement. However, the low strength of the materials and the small size but the large length-diameter ratio of the workpieces make the stiffness of micro-shafts low. The workpiece deformation still occurs, even if the cutting forces are small in the micro-shaft turning process, which causes the relieving amount error [10, 11]. It is difficult to guarantee the surface quality and geometric accuracy due to the above problems to be solved.

Factors impacting on the machining accuracy include geometric errors, thermal errors, cutting force deformation

✉ Pei Yan
pyan@bit.edu.cn

¹ School of Mechanical Engineering, Beijing Institute of Technology, No. 5 Zhongguancun South Street, Haidian District, Beijing 100081, People's Republic of China

² Key Laboratory of Fundamental Science for Advanced Machining, Beijing Institute of Technology, No. 5 Zhongguancun South Street, Haidian District, Beijing 100081, People's Republic of China

³ Aerospace System Engineering Shanghai, Shanghai 201108, China

errors, servo tracking errors, and so forth [12]. In the turning process, especially in the precision turning of large length-diameter ratio shafts, one of the most critical errors is related to workpiece deformation caused by cutting forces [13, 14]. Due to the size limitation, the device used in the traditional turning process of slender shafts, such as the center and the follow rest, is no longer applicable to the micro-shaft turning process. The micro-shafts are usually cantilevered in turning, and the stiffness of the end overhanging in the air is low, which is more prone to deformation under the cutting forces [15]. In addition, as the workpiece diameter is reduced, the difficulty is increased to achieve an accurate tool setting, and the tool setting error is gradually significant [16]. Much efforts have been devoted to the improvement of machining accuracy for micro-shaft manufacture. Lu et al. [17] developed a micro-lathe turning system. Bang et al. [18] constructed a five-axis micro-machine tool composed of three linear stages (X-, Y-, and Z-axis) and two rotary stages (A- and C-axis). An air motor micro-spindle with a maximum rotation speed of 30,000 rpm was chosen and fixed on a rotary stage (C-axis). Lim et al. [19] made an attempt to fabricate microstructures using a combination of turning and electrical-discharge machining (EDM). Guo et al. [20] presented an error compensation system including a fuzzy PID controller. The errors/inaccuracies can be reduced with the structural improvement of the machine tool through better design, manufacturing, and assembly practices. However, that method will result in very high manufacturing cost particularly when the accuracy requirements are beyond certain levels. Therefore, in order to avoid workpiece deformation or deflection and improve the machining accuracy of micro-shafts, force control and error compensation are the cost-effective method [21, 22]. The cutting forces must be limited within a range of less than the plastic deformation of the workpiece.

Accurate prediction of workpiece deformation with different process parameters is an essential part of error compensation work. The most important factor influencing the workpiece deformation or deflection is cutting forces. Hence, the coupling relation between the cutting forces and workpiece deformation must be taken into account. Lim et al. [19] reported that the thrust force was the main cause of workpiece deflection. And, the resultant force vector was gradually close to the thrust direction with the decrease of radial cut depth. Arsecularatne et al. [23] indicated that the chip flow direction and the cutting forces in oblique machining had relations with tool geometries, and the prediction models were developed. Xiao et al. [24] extended that tool nose radius had an influence on the residual stress distribution, surface finish, and tool wear. Sharman et al. [25] and Chen et al. [26] pointed out that the thrust force increase with tool nose radius

increasing. Therefore, it is extremely necessary to consider the tool nose radius when establishing the cutting force model.

The workpiece stiffness increases and the deflection decreases gradually when the tool is continuously approaching the chuck with a certain axial feed rate, wherefore the deformation errors are also different along the axis of the workpiece. It is very difficult to accurately detect the deformation in real time without the high-sensitivity detection device because micro-shaft turning is a typical dynamic machining process and the workpiece scale is small. For that case, the FEA method is regarded as a powerful and commonly used numerical method to simulate nonlinear/linear dynamic machining processes [27]. A lot of software packages used in metal cutting simulations have been developed, such as Abaqus/Explicit, DEFORM, and AdvantEdge [28]. The FEA method has been widely used to solve a number of complex engineering problems, such as the prediction of the cutting forces, chip deformation and surface integrity, thin-walled components deformation in the milling process, and cutting heat/temperature [29–31]. Not only prediction models based on FEA can reduce a lot of experiments but also the prediction results are close to the experimental consequence. Therefore, the FEA method provides an effective solution in adaptive control for machining processes, reducing machining errors and improving productivity and product quality [32]. In this paper, the FEA method is used to predict the dynamic deformation of the workpiece in micro-shaft turning by means of the analytical software ABAQUS/Explicit. An appropriate compensation strategy has been developed based on the simulation results subsequently to improve the machining accuracy of micro-shafts.

In order to improve the dimensional accuracy of micro-shafts manufactured with conventional precision machine tool for standardized and mass production, this paper proposed an error compensation strategy for the workpiece deformation error induced by cutting forces and tool setting error, which is based on the constant force cutting method and tool path planning. Organization for the remainder of this paper is as follows: in Section 2, an analysis model of micro-shaft turning machining errors and a specific cutting force model are established, and then, a compensation strategy for deformation error is proposed. In Section 3, the modeling process of the FEA method is introduced and the simulation results are discussed. Then, a series of turning experiments with altering processing parameters (spindle speed, feed rate, depth of cut) are carried out, while the experimental results are analyzed and discussed in Section 4. Finally, conclusions drawn from this research are given in Section 5.

2 Theoretical models and compensation strategy

2.1 Error analysis model

Ideally, the workpiece is approximately rigid and the tool datum plane is parallel to the radial plane of the workpiece, while the tool tip is at the same height as the workpiece axis. As shown in Fig. 1a, the distance between the tool setting point A and the cutting point B is the radial feed, which is equal to the actual depth of cut. R_0 is the reference radius and R_1 is the desired radius.

$$R_1 = R_0 - a_f \tag{1}$$

where a_f is the radial feed.

However, in micro-shaft turning, due to the small size of the workpiece, it is difficult to achieve an accurate tool setting. The machining deviation caused by the tool tip deviating from the horizontal plane of the workpiece axis is called the non-sensitive direction error, which is usually neglected in the common turning process. Furthermore, the deviation of workpiece deformation induced by cutting forces is called the cutting force deformation error, which is called deformation error for short, including deflection and elastic deformation of the workpiece. In micro-shaft turning, the small scale, large aspect ratio, and low rigidity of the workpiece make the deformation error the main error component.

At a certain instant of stable cutting, the tool-workpiece relative position is shown by the solid line contour in Fig. 1b. Point C is the initial position of the tool tip, which just contacts the surface of the workpiece without cutting and

deformation when performing the tool setting. Assuming that the height difference between the tool tip (point C) and the horizontal plane of the workpiece axis is Y_0 . When the tool tip feed from point C to point D along the X-axis, the workpiece is deflected by cutting force and the axis offsets from point O to point O'. According to the geometric relationship, the actual radius can be calculated:

$$R_2 = \sqrt{(X_2 - w_x)^2 + (Y_0 - w_y)^2} \tag{2}$$

$$X_2 = X_0 + a_f \tag{3}$$

where w_x and w_y are the radial deflection along the X-axis and the tangential deflection along the Y-axis respectively. a_f is the given cutting depth along the radial direction. X_2 and Y_0 are the horizontal and vertical coordinates of the tool tip D in the stable cutting state. And, X_0 is the horizontal coordinate of point C.

If only the deflection of the workpiece caused by the cutting forces is considered, as shown in Fig. 1c, the deflection curve function of the workpiece axis and the calculation formula for the deflection of the tool-workpiece contact point are as follows:

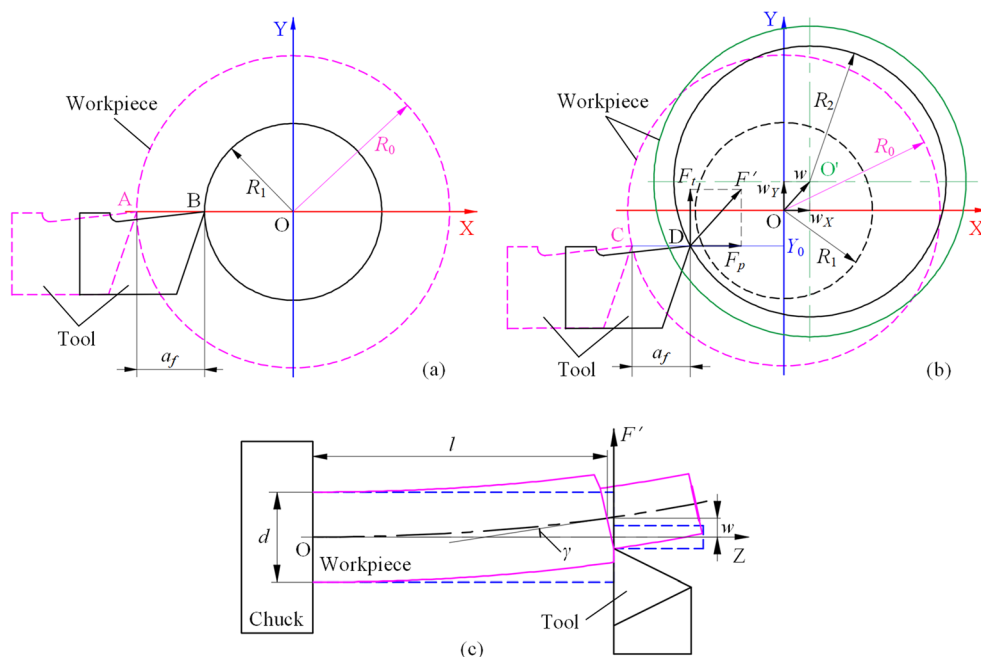
$$\omega(z) = \frac{32F'l^2z^2}{3\pi Ed^4}(3l-z) \tag{4}$$

$$l(t) = L - ft \tag{5}$$

$$w = \omega(l) = \frac{64F'l^3}{3\pi Ed^4} \tag{6}$$

where F' is the resultant force of the main cutting force F_t and the radial thrust force F_p , and l is the overhang length of the

Fig. 1 Machining error analysis diagram of micro-shaft turning with **a** ideal tool-workpiece relative position, **b** tool-workpiece relative position in reality, and **c** the deflection of workpiece induced by cutting forces



workpiece. t is the time to start cutting. L and f are the total length of workpiece and the feed rate along the workpiece axial respectively. E and d are Young's modulus and the diameter of the workpiece to be machined respectively.

The deflection components along X-axis and Y-axis can be calculated:

$$w_X = w \cos \varphi \quad (7)$$

$$w_Y = w \sin \varphi \quad (8)$$

$$\varphi = \arctan(F_t/F_p) \quad (9)$$

where φ is the angle between F_t and F_p .

Therefore, considering the influence of tool setting deviation and workpiece deflection error, the relative size error in one feed can be calculated:

$$\delta_1 = R_2 - R_1 = R_2 - R_0 - X_0 + X_2 \quad (10)$$

where R_0 is a reference radius for tool setting.

After the n th ($n = 1, 2, 3, \dots$) cutting without compensation, the formula of the cumulative size error δ_n is as follows:

$$\delta_n = R_{n+1} - R_0 - X_0 + X_{n+1} \quad (11)$$

$$X_{n+1} = X_0 + \sum_{k=1}^n a_{fk} \quad (12)$$

$$\delta_n = R_{n+1} - R_0 + \sum_{k=1}^n a_{fk} \quad (13)$$

where R_{n+1} is the workpiece radius and X_{n+1} is the horizontal coordinate of the tool tip after the n th ($n = 1, 2, 3, \dots$) feed. And, a_{fk} is the radial feed of the tool tip after the k th ($k = 1, 2, 3, \dots, n$) feed.

2.2 Cutting force model

In micro-shaft turning, the depth of cut is generally small, so the tool nose radius cannot be ignored when establishing the cutting force modeling. In a certain instant of stable cutting, the instantaneous undeformed cutting area and the cutting force analysis are shown in Fig. 2.

The instantaneous undeformed cutting area can be divided into two parts. The instantaneous cutting area S_1 in Fig. 2a is calculated by:

$$S_1 = \int_0^f \sqrt{r^2 - (z-r)^2} dz + \int_f^{r+\frac{f}{2}} \left[\sqrt{r^2 - (z-r)^2} - \sqrt{r^2 - (z-r-f)^2} \right] dz \quad (14)$$

where r is the tool nose radius, which is 200 μm by measuring.

And, the instantaneous cutting area S_2 is calculated by:

$$S_2 = f \times (a_p - r) \quad (15)$$

where a_p is the actual depth of cut along the radial direction in micro-shaft turning.

So, the instantaneous cutting area S is the sum of S_1 and S_2 :

$$S = S_1 + S_2 = \int_0^f \sqrt{r^2 - (z-r)^2} dz + \int_f^{r+\frac{f}{2}} \left[\sqrt{r^2 - (z-r)^2} - \sqrt{r^2 - (z-r-f)^2} \right] dz + f \times (a_p - r) \quad (16)$$

The length of the major cutting edge L and the angle θ are respectively calculated by:

$$L = a_p - r + \theta r \quad (17)$$

$$\theta = \pi - \cos^{-1} \left(\frac{f}{2r} \right) \quad (18)$$

Then, the resultant cutting force F can be obtained by:

$$F = \sigma_1 S + \sigma_2 L = \sigma_1 (S_1 + S_2) + \sigma_2 L \quad (19)$$

where σ_1 and σ_2 are the specific cutting force on the rake face and the major cutting edge respectively, and their units are N/mm^2 and N/mm .

The analysis of the resultant cutting force in the machine coordinate system is shown in Fig. 2b. The cutting forces are given by:

$$F_p = F \cos \alpha \sin \beta \quad (20)$$

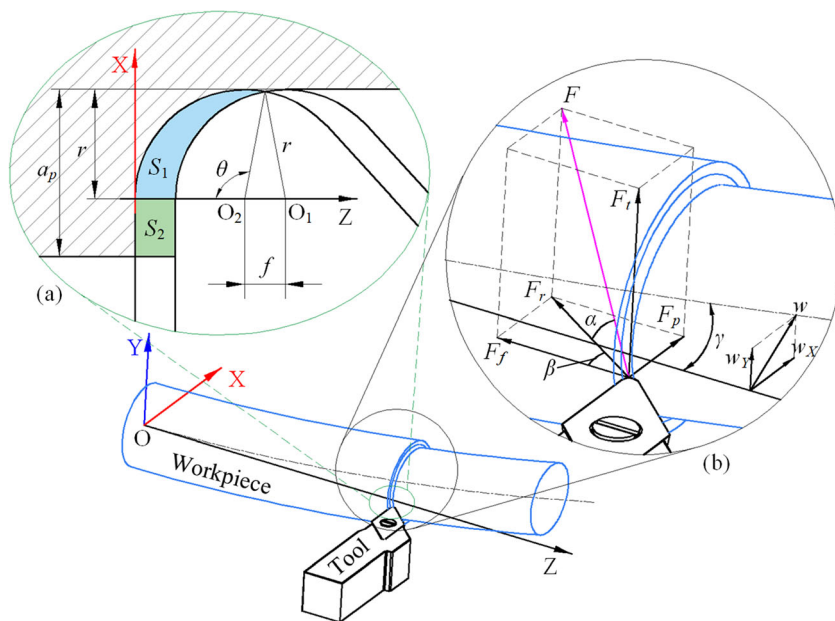
$$F_t = F \sin \alpha \quad (21)$$

$$F_f = F \cos \alpha \cos \beta \quad (22)$$

where F_p , F_t , and F_f are the radial thrust force along X-axis direction, the main cutting force along Y-axis direction and the axial thrust force along the Z-axis direction. α is the angle between force vector F and the XOZ plane and β is the angle between force vectors F_f and F_r .

Generally, the axial stiffness of the workpiece is better than other directions and the feed rate is low as well. Therefore, the influence of the axial thrust force F_f on workpiece deflection can be ignored, while the component forces in the other two directions are the analytical emphasis. When a set of cutting parameters (f and a_p , etc.) is given, S_1 , S_2 , S , and L can be calculated by Eqs. (14) to (16). The component forces along the X, Y, and Z-axis, F_p , F_t , and F_f in Fig. 2b, can be collected from a series of cutting force experiments, which has been done in the previous works. Then, the parameters like σ_1 , σ_2 , α , and β can be calculated by Eqs. (19) to (22), and the values are 889.6 N/mm^2 , 6.1 N/mm , 45.1°, and 56.4° respectively. Although the values of these parameters are only applicable to experiments in this paper, the calculation method is generic to all micro-shaft turning process.

Fig. 2 Schematic diagram of micro-shaft turning process with **a** the instantaneous undeformed cutting area and **b** the analysis of cutting forces in the space of machine coordinate system



2.3 Compensation strategy

According to the above analysis, when a precision machine tool is used for the turning process with a unified reference radius, the tool setting error is a fixed value that can be measured with laser measuring instrument, and the influence on the dimensional accuracy can be minimized with the help of precision tool setting system. However, the effects of workpiece deformation on machining accuracy are changing with the cutting parameters; the compensation for the deformation error should be taken into account. The tool-workpiece relative position, which is associated with the cutting parameters and the workpiece deformation, is an important factor determining the deformation error. If assuming that the workpiece in micro-shaft is regarded as a rigid shaft without deflection, only the deformation error is considered to be caused by the variable elastic position adjustment of the tool tip. Figure 3 is the equivalent schematic of Fig. 1b, and point E (X_1, Y_1) is the equivalent tool tip. The formula for calculating R_2 can be rewritten as:

$$R_2 = \sqrt{X_1^2 + Y_1^2} = \sqrt{(X_0 - a_t)^2 + (Y_0 - w_Y)^2} \tag{23}$$

$$a_t = X_2 - w_X \tag{24}$$

where a_t is the equivalent radial feed. Obviously, the deformation error is transformed into the radial feed deviation along the sensitive direction and the tool tip height deviation along the non-sensitive direction.

In the conventional turning process, the non-sensitive direction error is always neglected because of the little impact on the dimensional accuracy of the workpiece, and the sensitive direction error is the emphasis of error compensation. In order

to investigate whether there is the same regular pattern in micro-shaft turning, a set of non-sensitive direction deviation values $Y_0 = 0.1, 0.3, \text{ and } 0.5 \text{ mm}$ were substituted into Eq. (11) to draw the results in Fig. 4. It was found that as the diameter of the workpiece decreases, the influence of the non-sensitive direction deviation on the dimensional error becomes more and more significant. Thence, the compensation of non-sensitive direction error is important, especially in turning the micro-shaft with a diameter of less than 1 mm.

The stable and controllable depth of cut is an important precondition for ensuring continuous cutting and the machining accuracy in micro-shaft machining. In the conventional turning process, the cutting parameters are usually constant in a machining process. The cutting forces change with the unstable depth of cut, which is caused by an irregular shape of

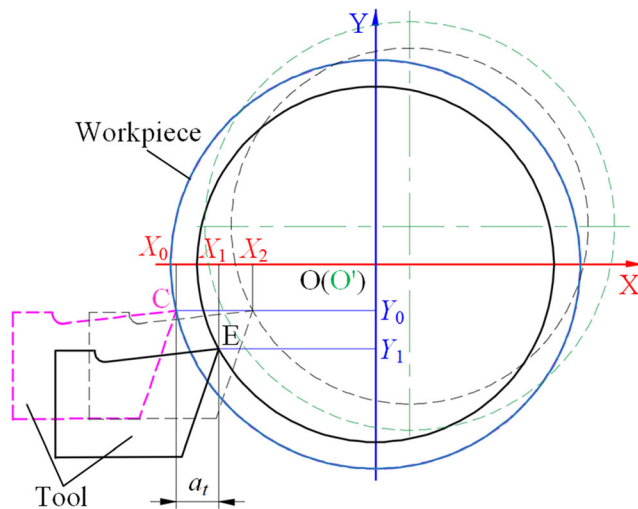


Fig. 3 The equivalent schematic of deformation error

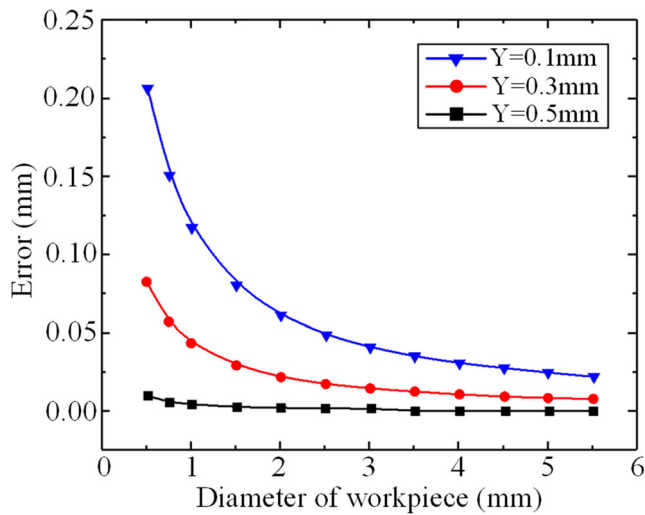


Fig. 4 Impact of workpiece diameter on deformation error along the non-sensitive direction

the blank and complex features of the workpiece to be machined making machining quality worse, cutting tools collapse, or even machine damage. In order to avoid this phenomenon, the constant force cutting technology based on the real-time cutting force monitoring was proposed, which keeps the cutting forces within a relatively stable range by means of monitoring the cutting forces real timely and adjusting the cutting parameters through machine control system after data analysis. The practice has proved that this method can improve productivity while ensuring machining accuracy and operational safety.

However, the main reason hindering its universal application includes the high cost of the high-sensitivity detection system and fast-response control system and the complexity of machine tool reformation. In addition, when the cutting force oscillation is detected, the damage has already generated, and the subsequent adjustment of the cutting parameters only prevents the damage from continuing to deteriorate.

Relatively, due to the small scale and the dynamic elastic deformation, it is very difficult to accurately detect the cutting force in real time for the micro-shaft turning process without the high-sensitivity detection device. If the quality inspection of the blank and the simulation of the cutting process are

realized before the turning process, the deformation induced by cutting force at any moment could be predicted in advance. Then, a set of cutting parameters are determined, and the tool path of stable cutting can be planned. This method not only achieves high-precision and high-efficiency machining but also reduces manufacturing costs because there is no need to purchase monitoring devices and modify machine tools. Based on the above analysis, the optimized tool path after compensation is a space curve in the workpiece coordinate system. The parametric equation of the tool tip point is developed, shown as Eq. (25).

$$\begin{cases} X(t) = X_0 + a_f + w(t)\cos\varphi \\ Y(t) = Y_0 + w(t)\sin\varphi \\ Z(t) = L-ft \end{cases} \quad (25)$$

According to the theoretical model and machining practice, cutting force is almost proportional to the depth of cut, while the actual depth of cut in turning is directly relevant to the final machining size and accuracy. Therefore, this paper considers that the idea of constant cutting force and the finite element analysis method can be used to plan the tool path with constant cutting depth, accordingly realizing the prediction and compensation of deformation in the micro-shaft turning process and improving the dimensional accuracy. The schematic diagram of the error compensation strategy is shown in Fig. 5.

Firstly, according to the dimensional accuracy requirements, the theoretical depth of cut is substituted into the cutting force prediction model mentioned in the previous section to estimate the cutting force components F_p , F_r , and F_f without considering the deformation of the workpiece. Secondly, the cutting force components are applied to the finite element model of the workpiece to simulate and calculate the deformation values of different positions along the workpiece axial with considering the material removal effects. Subsequently, the compensation amounts of tool path along the workpiece axial are calculated by means of the error analysis model. Finally, the trajectory of lathe tool based on actual follow-up cutting parameters is obtained and the G & M codes for controlling the machine tool servo system is programmed to adjust the tool-workpiece relative position in real time. After the

Fig. 5 Error compensation strategy of micro-shaft turning deformation based on the FEA method

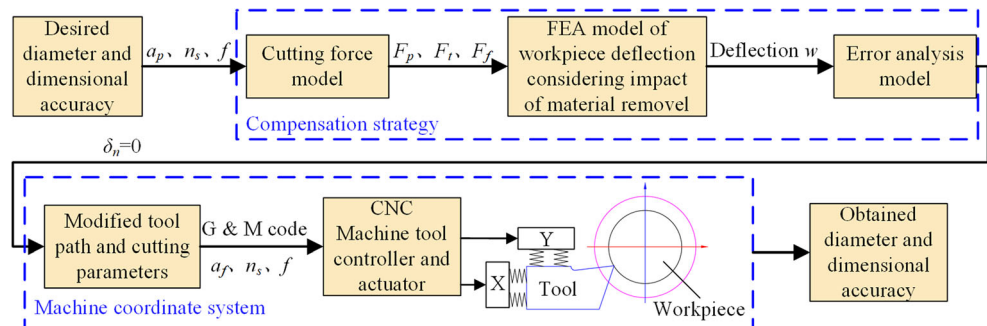


Table 1 Simulation material parameters of 7075 aluminum alloy

Elastic Modulus (MPa)	Poisson ratio	Density (kg/m ³)	Yield strength (25 °C/MPa)	Brinell hardness (kgf/mm ²)	Elongation rate
71000	0.33	2810	455	155	11

above operations, a micro-shaft with a more uniform size and higher precision can be got.

3 FEA-based modeling and simulation results

3.1 FEA-based prediction model of workpiece deformation

In general, when using a precision machine tool for the micro-shaft turning, the height deviation Y_0 between the initial tool tip point and the horizontal plane of the workpiece axis can be measured in the tool setting operation. But, the elastic deformation of the workpiece is dynamically changing with the cutting force in the turning process, which is difficult to measure online accurately. A FEA-based model of workpiece deformation, which is established by ABAQUS/Explicit to simulate the micro-shaft turning process, could not only quickly and accurately calculate the instantaneous deformation at any position of the workpiece with different processing parameters but also simulate and visualize the dynamic process of material removal.

According to the compensation strategy in the previous section (Fig. 5), the flowchart of modeling and simulating is shown in Fig. 6. Firstly, create the geometry model of the

workpiece and define material parameters. The material parameters in simulation analysis are shown in Table 1. Secondly, mesh the workpiece model with the medial axis algorithm according to feed per tooth and depth of cut, and number every element and node at the same time. The element type was defined as 3D stress and explicit dynamic analysis. Eight-node hexahedron reducing integral element (C3D8R) was chosen for all model elements, which has some advantages including the accurate solution to the displacement, difficult to occur shear self-locking under bending loads, and high computational accuracy with acceptable efficiency. Thirdly, define the boundary conditions. ENCASTRE boundary condition was used for constraining the six DOF of the workpiece clamping end, while a rotation boundary condition has been created and applied to the whole workpiece model. Subsequently, set every analysis step type as explicit dynamics and the step time equal to a single cutting step, which is equal to the reciprocal of the cutting speed.

When the first analysis step started, the number of the element to be removed at the free end was extracted and the calculated cutting forces were loaded on the corresponding element node step by step. The application process of cutting force is shown in Fig. 7. The workpiece deformation was

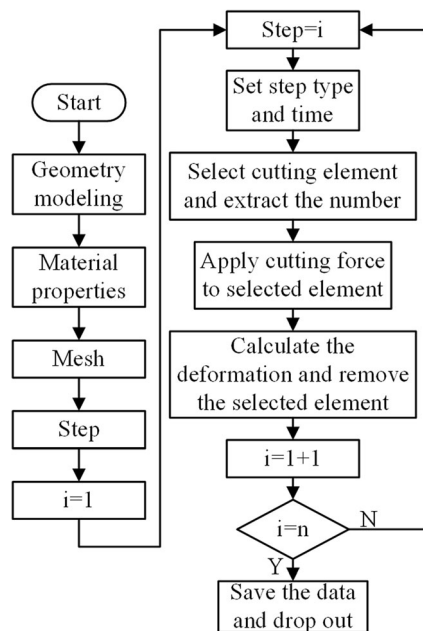


Fig. 6 The flow diagram of the FEA modeling

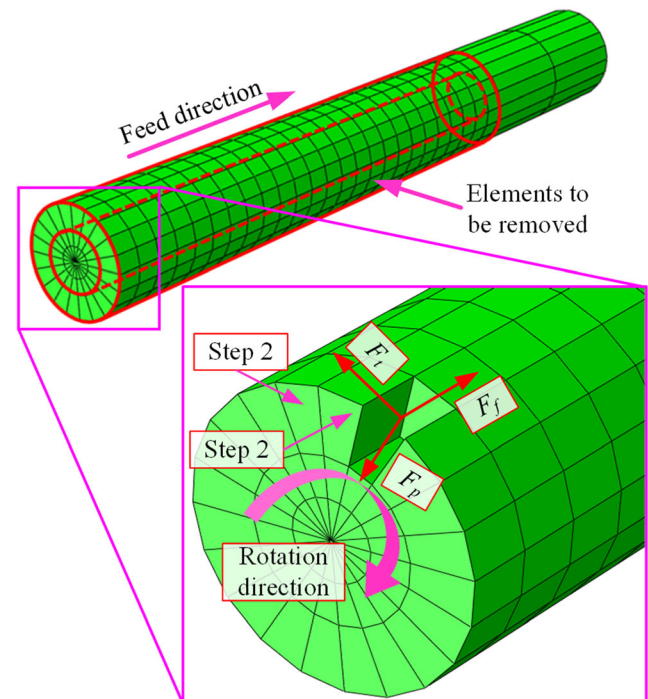


Fig. 7 3D finite element model and the application of cutting forces

Table 2 Parameters of FEM-based simulation and the cutting force calculation

Number	Diameter of the workpiece before turning (mm)	Depth of cut (mm)	Feed rate ($\mu\text{m/r}$)	Cutting speed (r/min)	F_t (N)	F_f (N)	F_p (N)
1	0.8	0.2	7	3000	1.85	1.06	4.54
2	1.2	0.4	7	3000	3.49	1.94	2.91
3	1.6	0.6	7	3000	5.28	2.93	4.40

calculated and the corresponding element was deleted. Then, continue the next analysis step and repeat until all the material in the cutting layer was removed. Finally, save the data of workpiece deformation and dropout. According to the calculation results, a tool path considering the influence of workpiece deformation could be got. Because there were numerous repetitive operations of cutting force applications and element deletions, after completing the preprocessing of the simulation model in software ABAQUS, the final INP files were completed with the help of an external rewrite program. Then, it was imported in ABAQUS/Explicit for submission and calculation.

The target part is a micro-shaft with a diameter of 0.4 mm and a length of 5 mm. The diameter of the workpiece before turning is from 0.8 to 1.6 mm, and the corresponding depth of cut is from 0.2 to 0.6 mm, which is much larger than the conventional micro-cutting, while the feed rate is small to ensure the instantaneous cutting area is appropriate. The

parameters of the finite element simulation and the cutting force values calculated from the prediction model in Section 2 are shown in Table 2.

3.2 Simulation result

The simulation process of micro-shaft turning is shown in Fig. 4, where L_t is the length of the cutting path. As can be seen from the figure, as the cutting progresses continuously, the closer to the workpiece clamping end, the smaller the amount of the workpiece deformation because of the high stiffness near the end of the workpiece clamping end. Meanwhile, the deviation of the workpiece free end is gradually reduced. The data of simulation deformation values is extracted from the ODB file by Python programming and plotted in a coordinate chart, of which the origin point of the horizontal coordinate represents the workpiece clamping end, while the vertical coordinate represents the deformation value, and the processes are shown in Figs. 8 and 9.

The finite element simulation results of Table 2 are shown in Fig. 10. The workpiece deformation increases rapidly with the decreasing of the distance between the workpiece clamping end and the cutting point, which is why the large

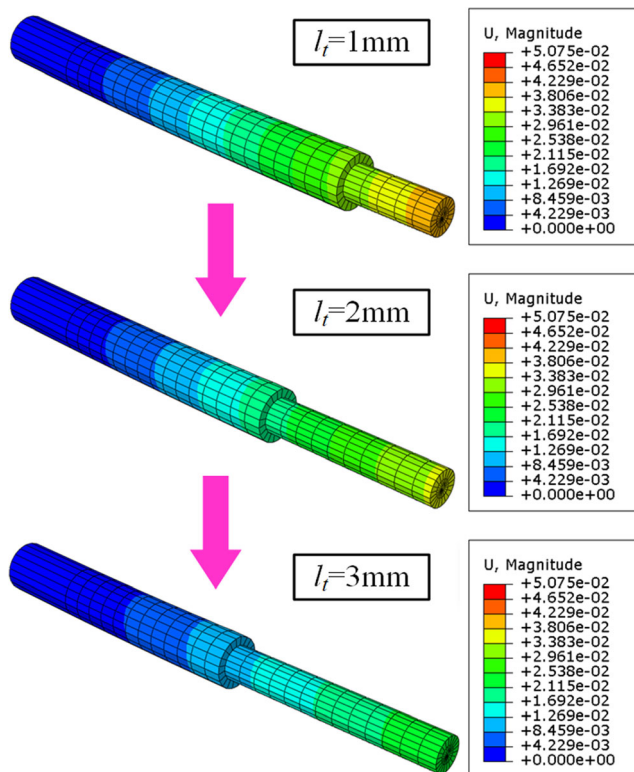
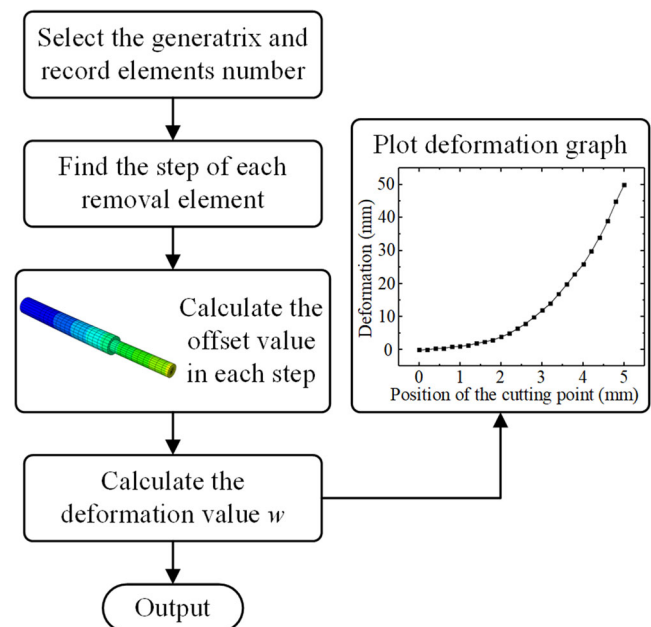
**Fig. 8** Process of finite element simulation**Fig. 9** The process of extracting the simulation deformation value

Fig. 10 Finite element simulation results of Table 2 with **a** number 1, **b** number 2, and **c** number 3

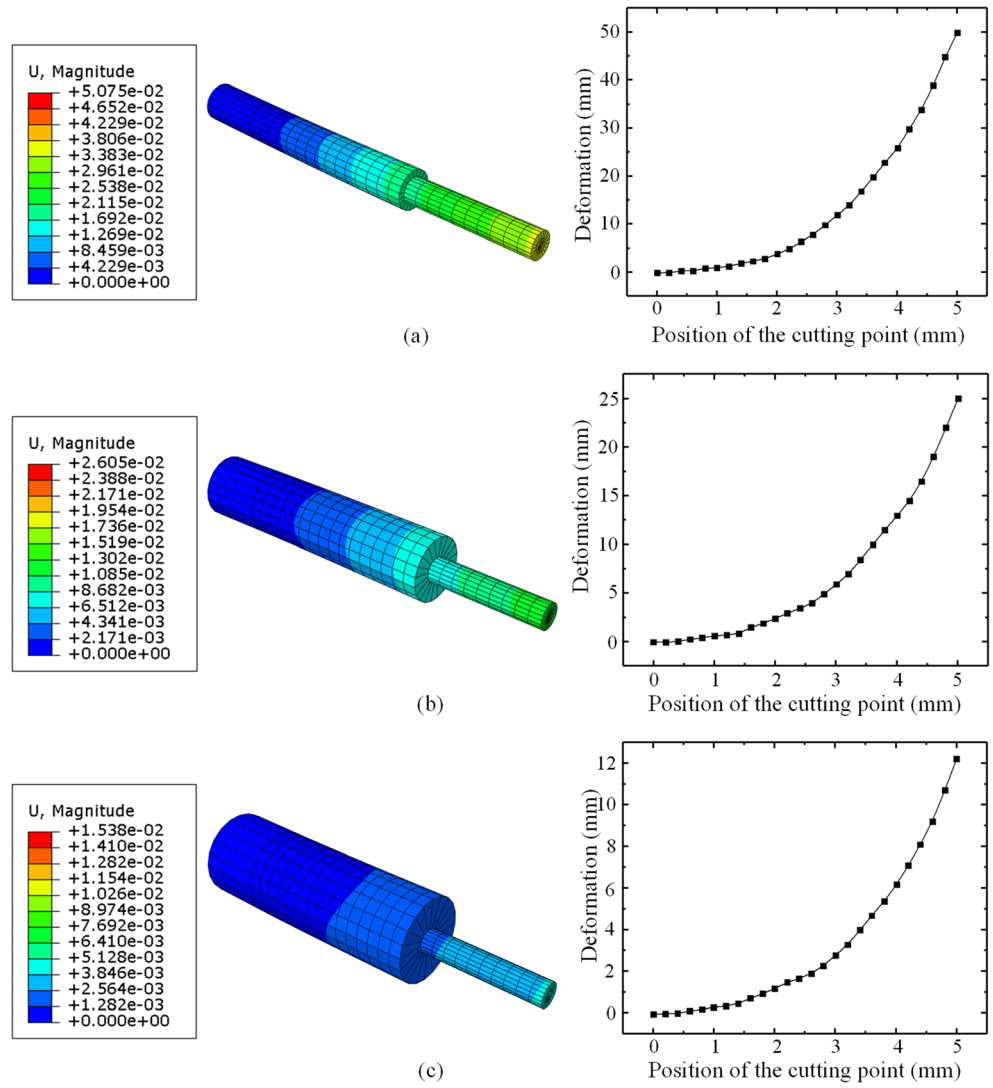


Fig. 11 The experiment process of micro-shaft turning

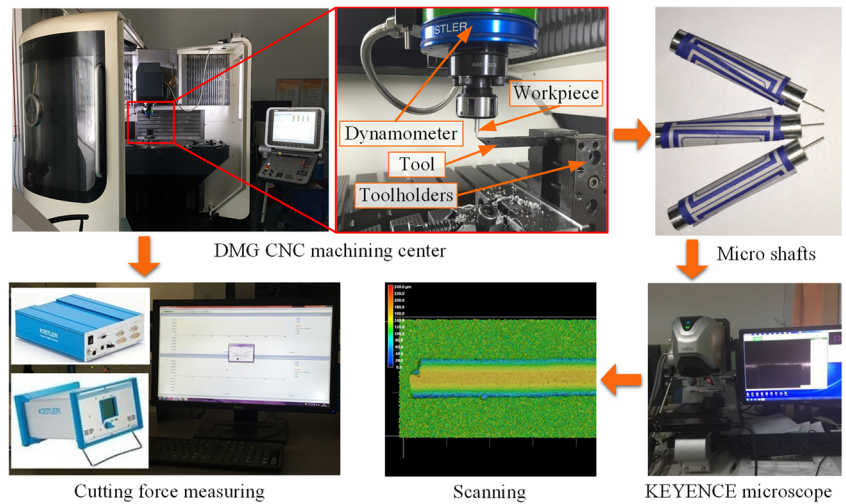


Table 3 The chemical composition of Al 7075

Chemical element	Si	Fe	Cu	Mn	Mg	Cr	Zn	Ti	Zr	Others
Content/%	0.12	0.15	2–2.26	0.1	5.28	2.93	4.40	0.006	0.08–0.15	0.15

length-diameter ratio shaft is difficult to machine. Comparing Fig. 10 a and b, when the diameter of the workpiece before turning increases by 50%, from 0.8 to 1.2 mm, the largest deformation value decreases by 51%, from 51 to 25 μm . Comparing Fig. 10 b and c, when the diameter of the workpiece before turning increases by 33%, from 1.2 to 1.6 mm, the largest deformation value decreases by 52%, from 25 to 12 μm . This means that when the diameter of the workpiece before turning increases, the workpiece stiffness increases faster than the cutting force.

4 Experiment design and result analysis

4.1 Experimental setup and processing parameters

According to the experimental requirements, the machine tool should have CNC programming function, high positioning accuracy, and sufficient operating space. Therefore, according to laboratory equipment conditions, the integral scheme of building an experimental platform is shown in Fig. 11. A precision CNC machining center, DMG 80 mono BLOCK, is used for the micro-shaft turning process experiment. The workpiece to be machined is clamped on the spindle, while the tool is fixed on the workbench. And, the relative position of tool-workpiece is adjusted by the machine tool servo system. The three-component piezoelectric rotating dynamometer, Kistler 5070A, is mounted on the machine spindle to record the cutting force during machining in real time. The 3D contour maps and the diameters of the machined micro-shafts are measured by KEYENCE microscope.

The workpiece is 7075 aluminum alloy bar and the chemical composition is listed in Table 3. The diameter of the blank before machining is uniform and large enough to guarantee the stiffness of the shaft so that the workpiece will not be broken in the turning process. The cutting tool used in the experiments is cemented carbide insert, which has strong wear resistance, reducing the adverse effects of tool wear on the results. The photo of the insert is shown in Fig. 12, and the geometric parameter information is listed in Table 4.

Table 4 The geometric parameters of the cutting tool

Tool material	Entering angle	Rake angle	Clearance angle	Tool nose radius
Cemented carbide	93°	0°	15°	200 μm

The experiments include two parts. Verifying the accuracy of the cutting force model and investigating the effects of cutting parameters on cutting force have been conducted in the first experiment, and the experimental parameters are shown in Table 5. Subsequently, contrast experiments are carried out to verify the effectiveness of the compensation strategy in the second experiment. The cutting parameters, which include depth of cut, the feed rate, and the spindle speed, are 0.3 mm, 7 $\mu\text{m}/\text{r}$, and 4500 r/min. The target diameter and length of micro-shaft are 0.4 mm and 5 mm respectively in both experiments.

4.2 Experiment results and discussion

Since the peak values of the cutting force signal in each sampling period can directly reflect the true values, the peak values are taken as the actual cutting force values. The original cutting force data collected by the dynamometer is plotted in the graph after filtering and noise reduction, as shown in Fig. 13.

The results of cutting force experiments based on the parameters in Table 5 are shown in Fig. 14, which are in good agreement with the results calculated by the cutting force prediction model. Since factors such as the strain hardening and the friction in the tool-workpiece interface are ignored for the purpose of simplifying calculations, the prediction values are slightly smaller than the experimental values. The maximum prediction error is less than 8.6%. Figure 14 a, b, and c correspond to the experimental numbers 1/2/3, 2/6/7, and 2/4/5, respectively, and the effects of feed rate, spindle speed, and depth of cut on main cutting force and radial thrust force are explored. It can be found that the effects of feed rate and depth of cut are more significant than spindle speed on cutting forces. Both the main cutting force and radial thrust force increase rapidly as feed rate and depth of cut increase but decrease slightly as spindle speed increases.

It can be explained from the cutting force model that cutting forces are directly related to the cutting area, while feed rate and depth of cut are two essential parameters in the calculation formulas of the cutting area, regardless of spindle

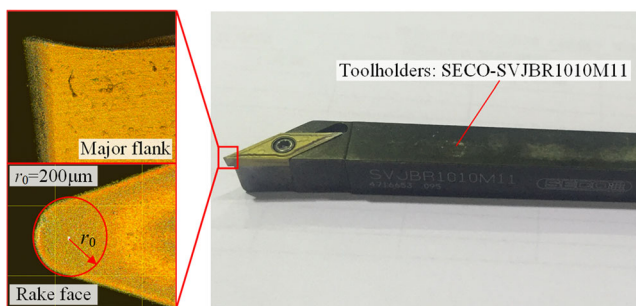


Fig. 12 The picture of the cutting tool

speed. However, the cutting speed increases very slowly as spindle speed increases because of the small scale of the workpiece. And, with spindle speed rising, the cutting forces go down because feed per revolution decreases.

After the contrast experiment to verify the effectiveness of the compensation strategy, the 3D contour maps and the diameters of the machined micro-shafts were measured by the KEYENCE microscope, as shown in Fig. 15a. The retracting point of the micro-shaft was selected as the measurement start point and the diameters are extracted every certain distance, as shown in Fig. 15b. The measurement results of workpieces machined without and with error compensation are plotted in Fig. 16 a and b, respectively, in which the horizontal axis represents the distance of the measurement point from the

measurement start point and the vertical axis represents the measured value of micro-shaft diameters at the picked points. In order to reduce measurement errors, each measurement point is repeated three times and take the average value as the final results.

As can be seen from Fig. 16, the machined error without compensation is much larger than that with compensation, especially away from the retracting point, like point B in Fig. 16a. The reason is that the cutter relieving phenomenon occurs because of the farther from the clamping end, the greater the elastic deformation, which makes the reduction of the actual cutting depth. The measured dimensions at point A are significantly smaller than the target diameter of 0.4 mm, which is most likely because of the accumulation of the material removed from the workpiece resulting built-up edge that causes overcutting. With the help of compensation, the dimensional error caused by the elastic deformation of the workpiece has been decreased by nearly 90%. However, due to the approximation in the prediction models and the complexity of the machining environment, the dimensional error caused by machining cannot be eliminated completely. Thence, there is still a small amount of dimension overshoot, like point C and point D in Fig. 16b, after compensation.

Table 5 Parameters of micro-shaft turning experiments

Experiment number	Diameter of the workpiece before turning (mm)	Depth of cut (mm)	Feed rate (µm)	Spindle speed (r/min)
1	1.4	0.5	2	3000
2	1.4	0.5	7	3000
3	1.4	0.5	30	3000
4	1.0	0.3	7	3000
5	2.4	1.0	7	3000
6	1.4	0.5	7	4500
7	1.4	0.5	7	6000

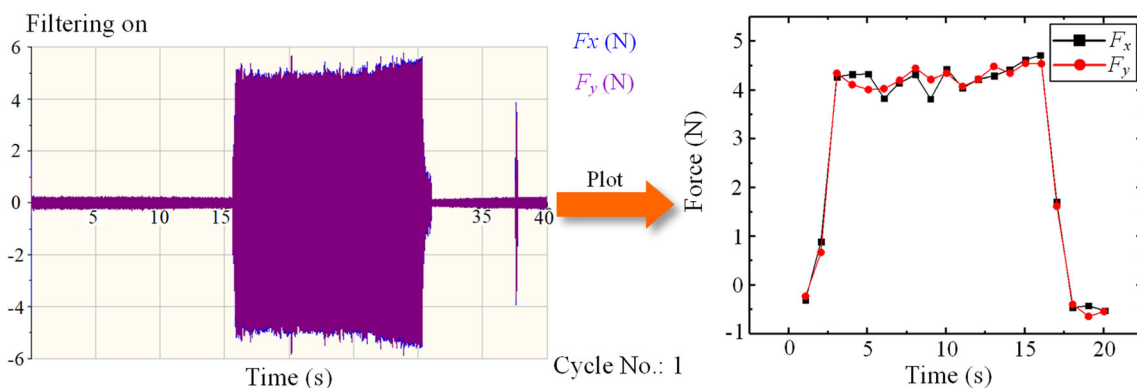


Fig. 13 Data processing of experimental cutting forces

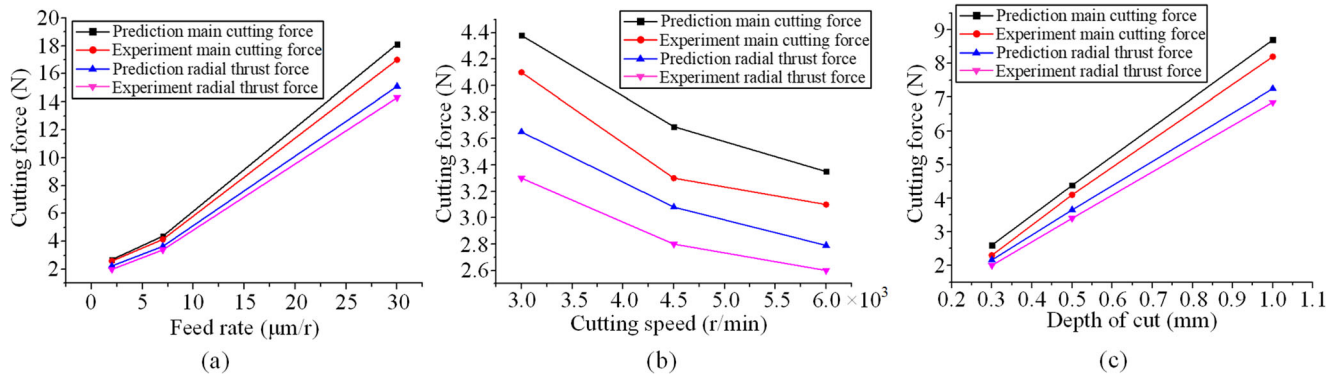


Fig. 14 Comparison of the cutting forces obtained by experiments and prediction model with the influence of feed rate in a, spindle speed in b, and depth of cut in c on main cutting force and radial thrust force

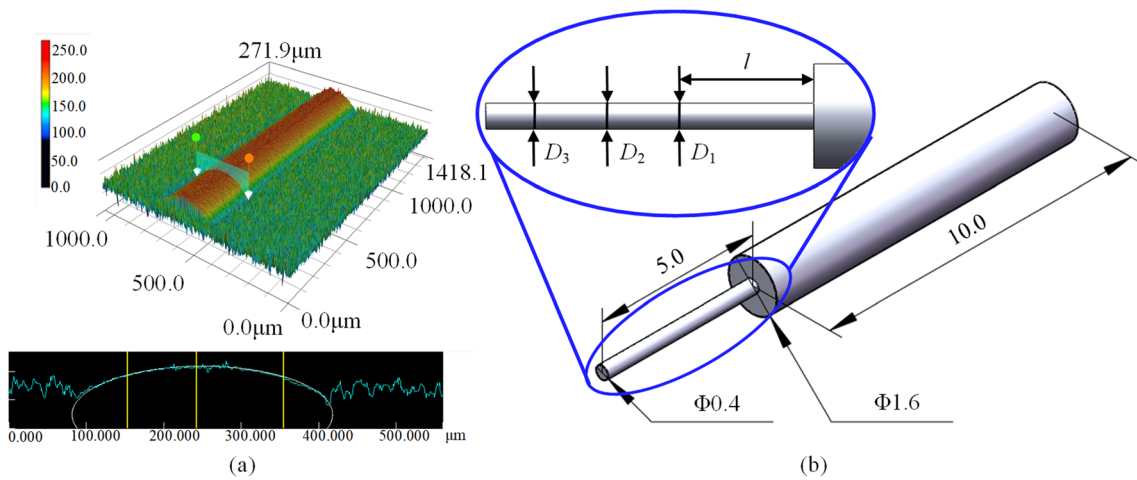
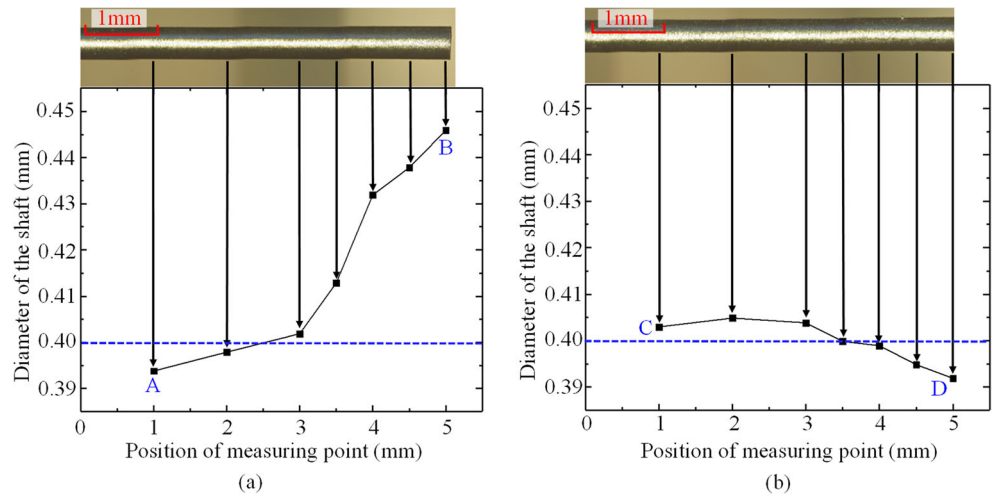


Fig. 15 The 3D contour maps of micro-shafts in a and the distribution of sample points in b

Fig. 16 Experimental results of micro-shaft turning process with a without compensation and b with compensation



5 Conclusions

Due to the small scale, large length-diameter ratio and the low stiffness of the micro-shaft parts, it is difficult to achieve accurate tool setting and monitor the workpiece deflection in real time. Based on the constant force cutting method and tool path planning, an error compensation method was proposed, which comprehensively considered workpiece deformation error induced by cutting forces and tool setting error. An error analysis model was established and a cutting force model considering the effect of tool nose radius as well as the FEA method has been applied to predict the compensation amounts. The feasibility of the error compensation method and factors affecting cutting forces has been researched by means of experiments. From the above research and discussion, the conclusions can be summarized as follows:

- (1) The non-sensitive direction error caused by tool setting and workpiece deflection cannot be ignored in analyzing and compensating the machining errors in the micro-shaft turning process. From the error analysis model, it was found that as the workpiece diameter decreases, the impact of the non-sensitive direction deviation on machining error becomes more and more significant.
- (2) Micro-shaft turning is a typical dynamic material removal process. With the situation of difficult to monitor the elastic deformation accurately, the FEA method is effective and convenient to estimate the compensation amounts and visualize the machining process. The simulation analysis results showed that the initial diameter of the workpiece has a much more significant effect on the workpiece deformation error than the radial depth of cut.
- (3) Compared with the experimental results, the maximum prediction error of cutting forces calculated through the specific cutting force model with given parameters is less than 8.6%. The constants in the cutting force model like σ_1 , σ_2 , α , and β were defined as 889.6 N/mm², 6.1 N/mm, 45.1°, and 56.4° respectively. According to the degree of influence on cutting forces, the cutting parameters were ordered as “feed rate > depth of cut > spindle speed,” from strong to weak.
- (4) Given a set of cutting parameters, the corresponding tool path could be planned. The contrast experiments have verified that the dimensional error of the micro-shaft with a large length-diameter ratio ($l = 5$ mm, $d = 0.4$ mm) was reduced by 90% with the compensation strategy.

The compensation strategy proposed in this paper is also suitable for improving the machining accuracy of micro-stepped shafts or other weak stiffness micro-parts. Further researches will be conducted on establishing more accurate prediction models and improve the accuracy of finite element simulation.

Funding information This work has been supported by the Natural Science Foundation of China (No. 51575050 and No. 51505034).

References

1. Qin Y (2015) Micromanufacturing engineering and technology (Second Edition): Chapter 1-Overview of micro-manufacturing. William Andrew publishing, pp 1–33
2. Goel S, Luo X, Agrawal A, Reuben RL (2015) Diamond machining of silicon: a review of advances in molecular dynamics simulation. *Int J Mach Tools Manuf* 88:131–164
3. Hourmand M, Sarhan AAD, Sayuti M (2016) Micro-electrode fabrication processes for micro-EDM drilling and milling: a state-of-the-art review. *Int J Adv Manuf Technol* 91:1023–1056
4. Alting L, Kimura F, Hansen HN, Bissacco G (2003) Micro engineering. *CIRP Ann* 52(2):635–657
5. Crichton ML, Archer-Jones C, Meliga S, Edwards G, Martin D, Huang H, Kendall MA (2016) Characterising the material properties at the interface between skin and a skin vaccination microprojection device. *Acta Biomater* 36:186–194
6. Chae J, Park SS, Freiheit T (2006) Investigation of micro-cutting operations. *Int J Mach Tools Manuf* 46(3-4):313–332
7. Li W, Liu MJ, Ren YH, Chen QD (2019) A high-speed precision micro-spindle use for mechanical micro-machining. *Int J Adv Manuf Technol* 102:3197–3211
8. Kumar GBV, Rao CSP, Selvaraj N, Bhagyashekar MS (2010) Studies on Al6061-SiC and Al7075-Al2O3 metal matrix composites. *J Miner Mater Charact Eng* 9(01):43–55
9. Shore Pand Morantz P (2012) Ultra-precision: enabling our future. *Philos Trans A Math Phys Eng* 370(1973):3993–4014
10. CH ZH (2016) Analysis on process of precision micro shaft parts. *Mech Mgmt Dev* 31(06):30–32
11. ZH ZY, Fang L (2015) Relieving amount error optimization research and application on dual-tools turning of slender shaft. *Mach Tool Hyd Raulics* 43(09):123–125
12. Fu G, Fu J, Xu Y, Chen Z, Lai J (2015) Accuracy enhancement of five-axis machine tool based on differential motion matrix: geometric error modeling, identification and compensation. *Int J Mach Tools Manuf* 89:170–181
13. Olvera D, De Lacalle LL, Compeán FI, Fz-Valdivielso A, Lamikiz A, Campa FJ (2012) Analysis of the tool tip radial stiffness of tum-milling centers. *Int J Adv Manuf Technol* 60(9-12):883–891
14. Shang GY, Deng ZP, Zhang ZY, Zhong L, Long J (2015) Research on dimension error of slender shaft in turning process. *J Chengdu Textile College* 32(01):19–21
15. Zhu MQ (2015) Research on turning-milling of low-rigidity workpieces. Dalian University of Technology, Dalian
16. Han QY, Hao J, Yu J, Dong G, Wang B (2016) Influence of tool sitting error upon precision of machining in NC turning. *Mach Build Autom* 45(1):61–63
17. Lu Z, Yoneyama T (1999) Micro cutting in the micro-manufacture turning system. *Int J Mach Tools Manuf* 39(7):1171–1183
18. Bang Y, Lee K, Oh S (2005) 5-axis micro milling machine for machining micro parts. *Int J Adv Manuf Technol* 25:888–894
19. Lim HS, Kumar AS, Rahman M (2002) Improvement of form accuracy in hybrid machining of microstructures. *J Electron Mater* 31(10):1032–1038
20. Guo JL, Chen LQ (2010) Error compensation in turning operation of slender shaft using a fuzzy PID controller. *Adv Mater Res Trans Tech Publ* 102:392–396
21. Senthilkumar V, Muruganandam S (2012) State of the art of micro turning process. *Int J Emerg Technol Adv Eng* 2:36–42

22. Mekid S, Ogedengbe T (2010) A review of machine tool accuracy enhancement through error compensation in serial and parallel kinematic machines. *Int J Precis Technol* 1(3–4):251–286
23. Arsecularatne JA, Mathew P, Oxley PLB (1995) Prediction of chip flow direction and cutting forces in oblique machining with nose radius tools. *Proc Inst Mech Engr B J Eng Manuf* 209(4):305–315
24. Xiao M, Sato K, Karube S, Soutome T (2003) The effect of tool nose radius in ultrasonic vibration cutting of hard metal. *Int J Mach Tools Manuf* 43(13):1375–1382
25. Sharman ARC, Hughes JI, Ridgway K (2015) The effect of tool nose radius on surface integrity and residual stresses when turning Inconel 718™. *J Mater Process Technol* 216:123–132
26. Chen W (2000) Cutting forces and surface finish when machining medium hardness steel using CBN tools. *Int J Mach Tools Manuf* 40(3):455–466
27. Nordgren A, Samani BZ, Saoubi RM (2014) Experimental study and modelling of plastic deformation of cemented carbide tools in turning. *Procedia CIRP* 14:599–604
28. Sadeghifar M, Sedaghati R, Jomaa W, Songmene V (2018) A comprehensive review of finite element modeling of orthogonal machining process: chip formation and surface integrity predictions. *Int J Adv Manuf Technol* 96(9–12):3747–3791
29. Pratap T, Patra K (2017) Finite element method based modeling for prediction of cutting forces in micro-end milling. *J Inst Engr (India) C* 98(1):17–26
30. Wan XJ, Hua L, Wang XF, Peng QZ, Qin XP (2011) An error control approach to tool path adjustment conforming to the deformation of thin-walled workpiece. *Int J Mach Tools Manuf* 51(3):221–229
31. Peng ZX, Li J, Yan P, Gao S, Zhang C, Wang X (2018) Experimental and simulation research on micro-milling temperature and cutting deformation of heat-resistance stainless steel. *Int J Adv Manuf Technol* 95(5–8):2495–2508
32. Arrazola PJ, Özel T, Umbrello D, Davies M, Jawahir IS (2013) Recent advances in modelling of metal machining processes. *CIRP Ann* 62(2):695–718

Publisher's note Springer Nature remains neutral with regard to jurisdictional claims in published maps and institutional affiliations.